ELSEVIER

Chemical Engineering Journal 82 (2001) 247–257

Chemical Engineering Journal

www.elsevier.com/locate/cej

Using CFD for scaling up gas–solid bubbling fluidised bed reactors with Geldart A powders

R. Krishna*, J.M. van Baten

Department of Chemical Engineering, University of Amsterdam, Nieuwe Achtergracht 166, 1018 WV Amsterdam, The Netherlands

Received 2 May 2000; accepted 13 October 2000

Abstract

The hydrodynamics of gas–solid fluidised bed are significantly affected by the scale of operation. This scale dependence is primarily caused by the scale dependence of the rise velocity of bubble swarms. Using the experimental data of Krishna et al. [Chem. Eng. Sci. 51 (1996) 2041–2050] for the bubble rise velocity, V_b, in air–FCC fluid beds of 0.1, 0.19 and 0.38 m diameter we develop a model for V_b using the Davies–Taylor–Collins relation as basis. This model is exactly analogous to that put forward earlier by Krishna et al. [Chem. Eng. Sci. 54 (1999) 171–183] for the rise of large bubble swarms in liquids. An Eulerian simulation model is developed for gas–solid fluid beds in which the drag between the (large) bubbles and the dense phase is calculated using the developed Davies–Taylor–Collins relations. Several simulations were carried out for columns ranging from 0.1 to 6 m in diameter. These simulations demonstrate the strong influence of column diameter on column hydrodynamics. The Eulerian simulation results rationalise the empirical correlation of Werther for the influence of column diameter on the bubble rise velocity V_b. The Eulerian simulation results are used to estimate the axial dispersion coefficients of the dense (emulsion) phase for columns ranging to 6 m in diameter; these are in agreement with the trends observed in the literature.

Keywords: Gas–solid bubbling; Fluidised bed reactors; Eulerian simulation model

1. Introduction

Gas–solid fluidised beds are difficult to scale up because of the strong influence of column diameter on the hydrodynamics and existing scale up procedures in the literature are largely empirical in nature [1–4]. The primary cause of the scale dependence of gas–solid fluid beds is the fact that the bubble rise velocity, V_b, is scale dependent. From the experimental data on V_b [1–4], it is clear that main factors influencing V_b are (a) average diameter of the bubble swarm, d_b (b) column diameter, D_T, and (c) height of the fluid bed, h. For a single, isolated, bubble of diameter d_b the rise velocity V_b^0 in a bed of powder is given by the Davies–Taylor relationship [5]

$$V_b^0 = 0.71\sqrt{gd_b} \tag{1}$$

This relationship is equally valid for the rise of spherical cap bubbles in liquids [6–11]. Due to the phenomenon of bubble growth, the average bubble diameter in a swarm increases with the height h above the distributor. Using a bubble-growth model, Darton et al. [12] derived the following relationship for the bubble diameter

$$d_b = 0.54\,(U - U_{df})^{2/5}\,(h + h_0)^{4/5}\,g^{-1/5} \tag{2}$$

where U is the superficial gas velocity and U_{df} is the velocity of gas through the dense (or emulsion) phase. The parameter h_0 characterises the distributor; for a porous plate distributor, for example, $h_0 = 0.03$ m. For fine Geldart A powders, the bubble growth does not take proceed indefinitely and the bubbles reach an equilibrium size, at a distance h^* above the distributor. The equilibration height h^* is determined inter alia by the particle size distribution. For fluid cracking catalyst ($d_p \approx 50\,\mu$m), h^* has a value of about 0.5 m [13] and the superficial gas velocity through the dense phase U_{df} has a value of about 2 mm/s, which is negligibly small in comparison with the operating gas velocities U used in this study. Clearly the phenomenon of bubble growth is important for short beds used in laboratory studies. In the experimental, and later computational, studies presented here we concentrate on the performance of fluid beds with dispersion heights ranging from 3 to 35 m (see Table 1), far in excess of the equilibration height of 0.5 m. In such cases the assumption of constant bubble diameter is justified. Above

* Corresponding author. Tel.: +31-20-525-7007; fax: +31-20-525-5604.
E-mail address: krishna@its.chem.uva.nl (R. Krishna).

1385-8947/01/$ – see front matter
PII: S1385-8947(00)00369-7

Nomenclature

AF	wake acceleration factor, dimensionless
C_D	drag coefficient, dimensionless
d_b	bubble diameter (m)
d_p	mean particle size (m)
D_T	column diameter (m)
$\boldsymbol{g}$	acceleration due to gravity (9.81 m s^{-2})
h	height above the gas distributor (m)
h^*	height above the gas distributor where the bubbles reach their equilibrium size (m)
h_0	parameter determining the initial bubble size at the gas distributor (m)
H, H_0, H_1	height of expanded bed, ungassed bed and after escape of dilute phase (m)
$\boldsymbol{M}$	interphase momentum exchange term (N m^{-3})
p	pressure (N m^{-2})
r	radial coordinate (m)
t	time (s)
$\boldsymbol{u}$	velocity vector (m s^{-1})
U	superficial gas velocity (m s^{-1})
$(U - U_{df})$	superficial gas velocity through the dilute phase (m s^{-1})
U_{df}	superficial velocity of gas through the dense phase (m s^{-1})
V_b	cross-section averaged rise velocity of the dilute phase (m s^{-1})
V_b^0	rise velocity of single, isolated, gas bubble (m s^{-1})
$V_b(r)$	radial distribution of the bubble velocity (m s^{-1})
$V_{df}(0)$	centre-line dense phase velocity (m s^{-1})
$V_L(0)$	centre-line liquid velocity in bubble column (m s^{-1})

Greek letters

ε	total gas voidage, dimensionless
ε_b	gas hold-up of "dilute" phase, dimensionless
ε_{df}	hold-up of gas in "dense" phase, dimensionless
μ_{df}	viscosity of dense phase (Pa s)
ρ_p	bulk and particle densities (kg m^{-3})
ρ_G, ρ_{df}	density of gaseous and dense phases (kg m^{-3})
ϑ	parameter defined in Eq. (3)
τ	stress tensor (N m^{-2})

Subscripts

b	referring to "dilute" or "bubble" phase
df	referring to "dense" phase
G	referring to gas phase
k,l	referring to k and l phases
T	tower or column

the initial "growth" zone, the coalescence and break-up processes are assumed to be in equilibrium.

Eq. (1) applies to the case where the bubble is far removed from the walls. In narrow columns, V_b is strongly influenced by wall effects; these wall effects decrease as the column diameter increases. The ratio of the bubble diameter to the column diameter, (d_b/D_T), is an important determinant in the estimation of V_b because this ratio determines the proximity of the bubbles to the wall. It is for this reason that the correlation of Werther [2] for the rise velocity V_b contains the influence of the column diameter in the form of a power-law function

$$V_b = 0.8(U - U_{df}) + 0.71\vartheta\sqrt{gd_b}; \quad \vartheta = 3.2D_T^{0.33} \tag{3}$$

The measurements of Werther were restricted to columns smaller than 1 m and the extrapolation of Eq. (3) to column diameters larger than 1 m is open to question. Werther suggests that we assume, without firm evidence, that the value of V_b does not increase beyond $D_T = 1$ m, i.e.

$$\vartheta = 3.2 \quad \text{for } D_T > 1\,\text{m} \tag{3a}$$

The purpose of the present communication is to develop a Computational Fluid Dynamics (CFD) model in order to describe the scale dependence of fluid beds. The strategy we adopt is to first develop a more fundamentally based model for the bubble rise velocity taking account of wall effects. This information is then incorporated into a CFD model using the Eulerian framework. Eulerian simulations are then used to study the scale (i.e. increasing column diameter) influence of fluid beds. We restrict our discussion to *bubbling* gas–solid fluidised beds of *fine* Geldart A powders without internals.

2. Development of model for bubble rise velocity

In order to develop a more fundamentally based model for the bubble rise velocity, we make use of the extensive set of experimental data developed earlier in our laboratories [4,13]. The experimental work was carried out in three columns made of polyacrylate sections. The column diameters were 0.1, 0.19 and 0.38 m with total heights of 3 or 4 m. Sintered plate gas distributors were used in these three columns. Two-stage cyclones were used to recover entrained fine particles and return these to the column. For the range of superficial gas velocities used in our experiments (0–0.4 m/s), the entrainment of fine particles in the freeboard region had no significant effect on the bed hydrodynamics. In all cases the pressure at the top of the column was close to atmospheric pressure. The gas inlet pipe at the bottom of the column was equipped with a quick shut-off valve for the purpose of performing dynamic gas disengagement experiments. Air was used as the gas phase in the experiments. The solid phase consisted of fluidised cracking catalyst (FCC) ($\rho_{bulk} = 960$ kg/m^3; $\rho_p = 1480$ kg/m^3; particle size distribution: 10% < 23 μm, 50% < 49 μm, 90% < 89 μm). The

Table 1
Column configurations, systems, operating conditions and grid details of CFD simulations of air–FCC[a]

Column diameter D_T (m)	Column height (m)	Initial dense phase height (m)	Observation height (m)	Number of grid cells (radial) × (axial)	Superficial gas velocity, U (m/s)
0.19	3	1.9	1.6	30 × 160	0.09, 0.16, 0.23, 0.3
0.38	3	1.9	1.6	30 × 160	0.09, 0.16, 0.23, 0.3, 0.35, 0.4
1.5	8	5.3	4	75 × 410	0.09, 0.16, 0.3
2	13	10	9	75 × 270	0.16, 0.3
4	25	20	18	75 × 510	0.16, 0.3
6	35	25	23	75 × 710	0.16, 0.3

[a] The bubble phase was injected over the central 13 (or 32) of the 30 (or 75) grid cells. The reported dense phase velocity profiles are at the observation heights reported below. The reported values of the total gas hold-up refer to the fractional gas volume below this observation height.

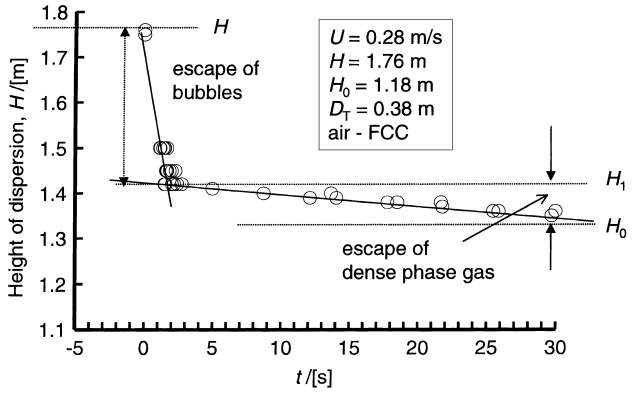

Fig. 1. Typical dynamic gas disengagement experiment for air–FCC in a 0.38 m diameter column.

unexpanded bed height ranged from $H_0 = 0.1$ to 1.5 m. For settled bed heights exceeding 1 m, it was established that the bubbles had reached their equilibrium bubble size within a distance of 0.5 m above the distributor. The superficial gas velocity U was in the range 0.001–0.65 m/s. Further details of our experimental set-up and procedure are available in our earlier publications [4,13].

A typical dynamic gas disengagement experiments with air–FCC in the 0.38 m diameter column is shown in Fig. 1. The initial sharp decrease in the bed height is due to escape of the fast-rising bubbles ("dilute" phase). When all the bubbles have disengaged, the gas in the emulsion or "dense" phase escapes. The slope of the second part of the curve can be used to determine the superficial gas velocity of the gas through the dense phase, U_{df}. The *total gas voidage*, or hold-up for G–S fluid bed was calculated from $\varepsilon = (H - \rho_{bulk} H_0/\rho_p)/H$. The *gas hold-up of the "dilute" phase*, ε_b, is determined from $\varepsilon_b = (H - H_1)/H$. The *gas voidage in the "dense" phase* is $\varepsilon_{df} = (\varepsilon - \varepsilon_b)/(1 - \varepsilon_b)$. For a range of gas velocities the dense phase gas voidage remains practically constant and is also independent of the column diameter. The superficial gas velocity through the dense phase, U_{df} is about 2 mm/s and therefore for the range of superficial gas velocities involved in industrial operations, we may take $(U - U_{df}) \approx U$. The rise velocity of the bubbles, i.e. dilute phase can be determined from $V_b \equiv (U - U_{df})/\varepsilon_b$. The bubble rise velocity data for settled bed heights greater than 1 m are shown in Fig. 2 for the three column diameters. The strong influence of the bed diameter is evident.

In order to develop a fundamental model for the bubble rise velocity in a gas–solid fluid bed we need to take account of the influence of the column diameter on the rise velocity by introducing a scale factor correction into the Davies–Taylor relation

$$V_b^0 = 0.71\sqrt{g d_b}(\mathrm{SF}) \tag{4}$$

where the superscript 0 is used to emphasize that the rise velocity refers to that of a single, isolated, bubble. Collins [14] has determined the scale correction factor for gas–liquid

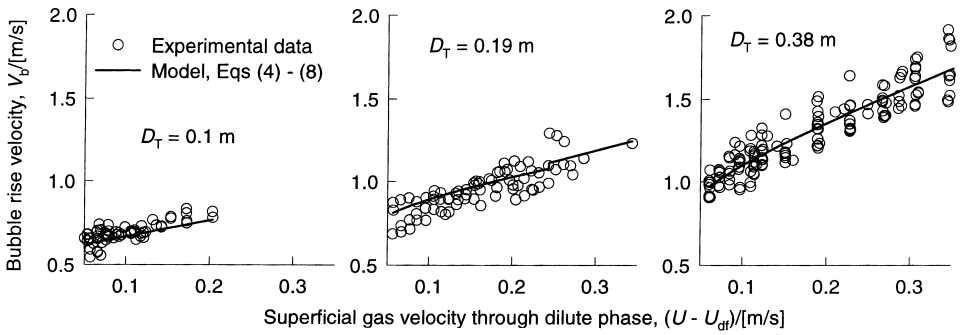

Fig. 2. Influence of superficial gas velocity through dilute phase and column diameter on the dilute phase rise velocity in gas–solid fluidised beds.

systems

$$\mathrm{SF} = \begin{cases} 1 & \text{for} \dfrac{d_\mathrm{b}}{D_\mathrm{T}} < 0.125 \\ 1.13 \exp\left(-\dfrac{d_\mathrm{b}}{D_\mathrm{T}}\right) & \text{for} \, 0.125 < \dfrac{d_\mathrm{b}}{D_\mathrm{T}} < 0.6 \\ 0.496\sqrt{\dfrac{D_\mathrm{T}}{d_\mathrm{b}}} & \text{for} \dfrac{d_\mathrm{b}}{D_\mathrm{T}} > 0.6 \end{cases} \quad (5)$$

We assert the validity of Eq. (5) for gas–solid fluid beds and shall seek validation later on in the paper.

The rise velocity in a bubble swarm will be higher than that of a single gas bubble due to wake interactions [8]. A bubble that gets into the wake of a preceding bubble gets accelerated. Such acceleration effects are observed in both gas–liquid systems [15–17] and gas–solid systems [18]. In order to take account of such wake interaction effects we introduce a multiplying factor, AF, which is the wake acceleration factor

$$V_\mathrm{b} = V_\mathrm{b}^0(\mathrm{AF}) = 0.71\sqrt{g d_\mathrm{b}}(\mathrm{SF})(\mathrm{AF}) \quad (6)$$

The acceleration factor, AF can be expected to be dependent on the average distance of separation between the bubbles; the smaller the separation, the greater the acceleration effect. The average distance of separation between the bubbles decreases with increasing superficial gas velocity through the dilute phase, $(U - U_\mathrm{df})$, and therefore the factor AF can be expected to increase with increasing values of $(U - U_\mathrm{df})$. We fitted the experimental data set for V_b for the 0.1, 0.19 and 0.38 m diameter columns with the Eqs. (4)–(6) to obtain expressions for the wake acceleration factor AF and the bubble size d_b. The regressed relations yielded the following expressions

$$\mathrm{AF} = 1.64 + 2.7722(U - U_\mathrm{df}) \quad (7)$$

$$d_\mathrm{b} = 0.204(U - U_\mathrm{df})^{0.412} \quad (8)$$

We note that the bubble rise velocity in a gas–solid fluid bed are about 1.5–3 times higher than the rise velocity of a single gas bubble, given by Eq. (4), underlining the strong wake interaction effects. The predictions of the model given by Eqs. (4)–(8) are compared with the measured data in Fig. 2. The fit is very good for all three columns studied experimentally, confirming the validity of the Collins relations for gas–solid fluid beds.

The fitted bubble size correlation (8), shown in Fig. 3, matches extremely closely with the values calculated from the Darton et al. [12] bubble growth formula (2) taking the bed height h to be 0.5 m and $h_0 = 0.03$ m for porous plate distributors; see the dashed line in Fig. 3. The experimental results can be rationalised by assuming that the bubbles reach their equilibrium bubble size at a distance 0.5 m above the distributor. In reality there is a distribution of bubble sizes and the fitted d_b represents an average value. Eqs. (4)–(8) are sufficient to allow calculation of the dilute phase rise velocity in a fluidised bed.

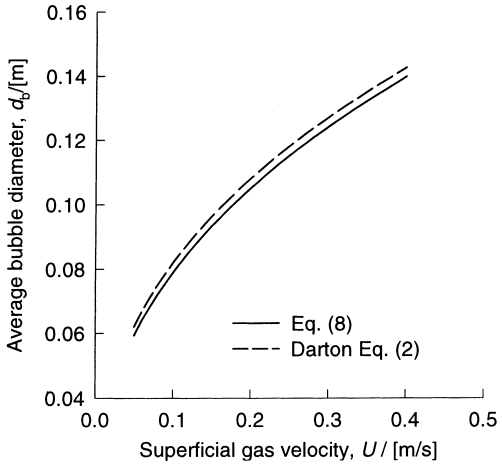

Fig. 3. Bubble size estimation for gas–solid fluid beds.

3. Eulerian simulations of gas–solid fluidised beds

In recent years, there has been considerable academic and industrial interest in the use of computational fluid dynamics (CFD) to model gas–solid fluidised beds. CFD modeling of fluidised beds usually adopts the Eulerian framework for both the dilute and dense phases and makes use of the granular theory to calculate the dense phase rheological parameters [19–29]. The granular theory can be successfully applied for relatively coarse Geldart B powders and its extension to Geldart A powders poses several problems with respect to the proper modeling of interparticle collision and interaction [22]. Discrete particle Langrangian simulations of the particle phases have also been attempted [30] but the computational load is such that it cannot be used for design and scale up purposes. Our approach here will be to treat the "dense" phase in a fluid bed as a pseudo-fluid (liquid). With this approach the Eulerian simulations become identical, in principle, to that of bubble columns albeit with different interphase momentum exchange characteristics [31–43].

The two-phase model [1–4] underlies our approach, wherein lumped phases "dilute" and "dense" are defined as shown and ascribed fluid properties. For the air–FCC system we estimate the "dense" phase viscosity μ_df to be 0.125 Pa s, using the data summarized by Yates [44]. The density of the dense phase ρ_df was estimated from the experimental data to be 830 kg m^{-3}.

For each of the "dilute" and "dense" phases shown, the volume-averaged mass and momentum conservation equations are given by

$$\frac{\partial \varepsilon_k \rho_k}{\partial t} + \nabla \cdot (\varepsilon_k \rho_k \boldsymbol{u}_k) = 0 \quad (9)$$

$$\frac{\partial (\varepsilon_k \rho_k \boldsymbol{u}_k)}{\partial t} + \nabla \cdot (\varepsilon_k \rho_k \boldsymbol{u}_k \boldsymbol{u}_k) = -\varepsilon_k \nabla_p + \nabla \cdot (\varepsilon_k \tau_k) + \boldsymbol{M}_{kl} + \varepsilon_k \rho_k \boldsymbol{g} \quad (10)$$

where ρ_k, $\boldsymbol{u}_k$, ε_k and τ_k represent, respectively, the macroscopic density, velocity, volume fraction and stress tensor of the kth phase, p is the pressure, $\boldsymbol{M}_{kl}$, the interphase momentum exchange between phase k and phase l and $\boldsymbol{g}$ is the gravitational force. For the continuous, dense, phase, the turbulent contribution to the stress tensor is evaluated by means of $k-\varepsilon$ model, using standard single phase parameters, $C_\mu = 0.09$, $C_{1\varepsilon} = 1.44$, $C_{2\varepsilon} = 1.92$, $\sigma_k = 1$ and $\sigma_\varepsilon = 1.3$. The dilute (bubble) phase, which is the dispersed phase, is assumed to be in laminar flow. It was also determined from CFD simulations that the assumptions regarding the flow field inside the bubbles were not crucial. The momentum exchange between the dilute (subscript b) and dense (subscript df) phases is given by

$$\boldsymbol{M}_{\mathrm{df,b}} = \frac{3}{4}\rho_{\mathrm{df}}\frac{\varepsilon_{\mathrm{b}}}{d_{\mathrm{b}}}C_D(\boldsymbol{u}_{\mathrm{b}} - \boldsymbol{u}_{\mathrm{df}})|\boldsymbol{u}_{\mathrm{b}} - \boldsymbol{u}_{\mathrm{df}}| \tag{11}$$

The interphase drag coefficient is calculated from

$$C_{\mathrm{D}} = \frac{4}{3}\frac{\rho_{\mathrm{df}} - \rho_{\mathrm{G}}}{\rho_{\mathrm{df}}}gd_{\mathrm{b}}\frac{1}{V_{\mathrm{b}}^2} \tag{12}$$

where the rise velocity of the dilute phase V_{b} is given by the Eq. (4). The wake acceleration factor AF and the bubble size d_{b} are calculated using Eqs. (7) and (8). The assumption of constant bubble size along the height of the column is an important limitation and the results of the simulation are expected to apply to describe the hydrodynamics of tall commercial scale reactors with a high height to diameter ratio. We have only included the drag force contribution to $\boldsymbol{M}_{\mathrm{df,b}}$, in keeping with the papers on gas–liquid bubble columns [37–43]. Other forces such as added mass, lift, Magnus and Saffmann are ignored in the present analysis [33]. Furthermore, our CFD model ignores mass transfer between the dilute and dense phases and any chemical reaction in the dense phase.

A commercial CFD package CFX 4.1c of AEA Technology, Harwell, UK, was used to solve the equations of continuity and momentum for the two-fluid mixture. This package is a finite volume solver, using body-fitted grids. The grids are non-staggered and all variables are evaluated at the cell centres. An improved version of the Rhie–Chow algorithm [45] is used to calculate the velocity at the cell faces. The pressure–velocity coupling is obtained using the SIMPLEC algorithm [46]. For the convective terms in Eqs. (9) and (10) hybrid differencing was used. A fully implicit backward differencing scheme was used for the time integration.

Several column configurations were simulated as specified in Table 1. For a chosen set of operating conditions and column diameter the bubble size d_{b} and the corresponding drag coefficient C_{D} were calculated using Eq. (12).

In the CFD literature, two types of simulations have been attempted: (a) two-dimensional axi-symmetric simulation (in cylindrical coordinates) and (b) a fully three-dimensional simulation [38]. We first examine the validity of 2D axi-symmetry by comparison with a complete 3D simulation for a highly viscous liquid, Tellus oil ($\rho_{\mathrm{L}} = 862\,\mathrm{kg/m^3}$; $\mu_{\mathrm{L}} = 0.075\,\mathrm{Pa\,s}$; $\sigma = 0.028\,\mathrm{N/m}$). The hydrodynamics of a bubble column with Tellus oil is extremely close to that of a fluid bed with FCC particles (we verify this towards the end of this paper). For comparison of 2D and 3D results, the transient 3D data for hold-ups and velocities were time averaged (using the last 2000 time steps) and spatially averaged in the azimuthal direction [38]. Fig. 4(a) compares the radial distribution of liquid velocity obtained with 2D and 3D simulations for a column of 0.38 m diameter column operating at a superficial gas velocity of 0.23 m/s. We note that the profiles are comparable in magnitude and in good agreement with experimentally determined profiles (details in [39]; see Fig. 4(b)). In Fig. 5 the centre-line liquid velocity $V_{\mathrm{L}}(0)$ from 2D simulations obtained for a range of superficial gas velocities are compared with experimental data. We see that the agreement is very good. Fig. 6 compares the radial distribution of gas hold-up predicted by 2D and 3D simulations. We note that the assumption of

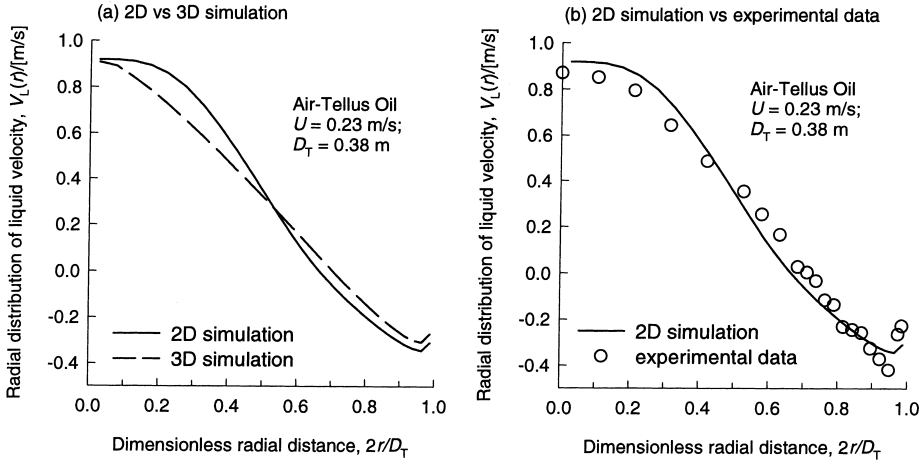

Fig. 4. Radial distribution of liquid velocity for air–Tellus oil in a 0.38 m diameter column operating at $U = 0.23$ m/s. (a) Comparison of 2D axi-symmetric with 3D simulations. (b) Comparison of experimental data with 2D simulations; details in [38,39].

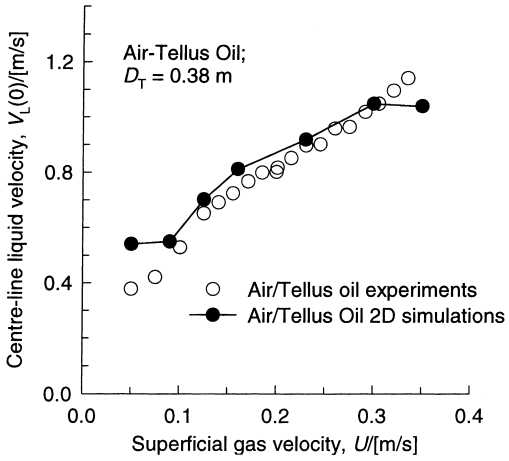

Fig. 5. Comparison of experimental centre-line velocity data on $V_L(0)$ for air–Tellus oil systems in 0.38 m diameter column with 2D axi-symmetric simulations; details in [38,39].

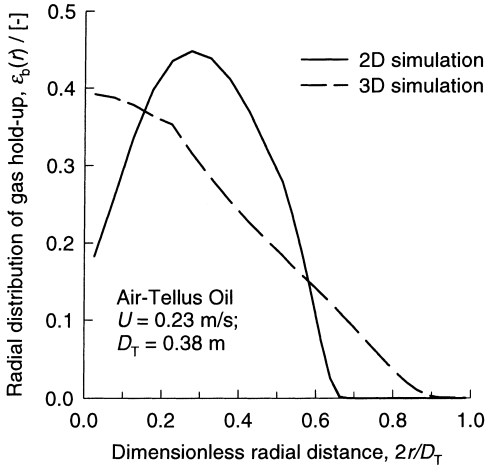

Fig. 6. Radial distribution of gas hold-up for air–Tellus oil in a 0.38 m diameter column operating at $U = 0.23$ m/s. Comparison of 2D axi-symmetric with 3D simulations.

cylindrical axi-symmetry prevents lateral motion of the dispersed bubble phases and leads to an unrealistic gas bubble hold-up distribution wherein a maximum hold-up is experienced away from the central axis. In the 3D simulations, on the other hand, in which lateral motion in both radial and azimuthal directions are catered for, yield physically realistic distribution of gas hold-ups, and are in reasonably good agreement with experiment. Despite the unrealistic gas

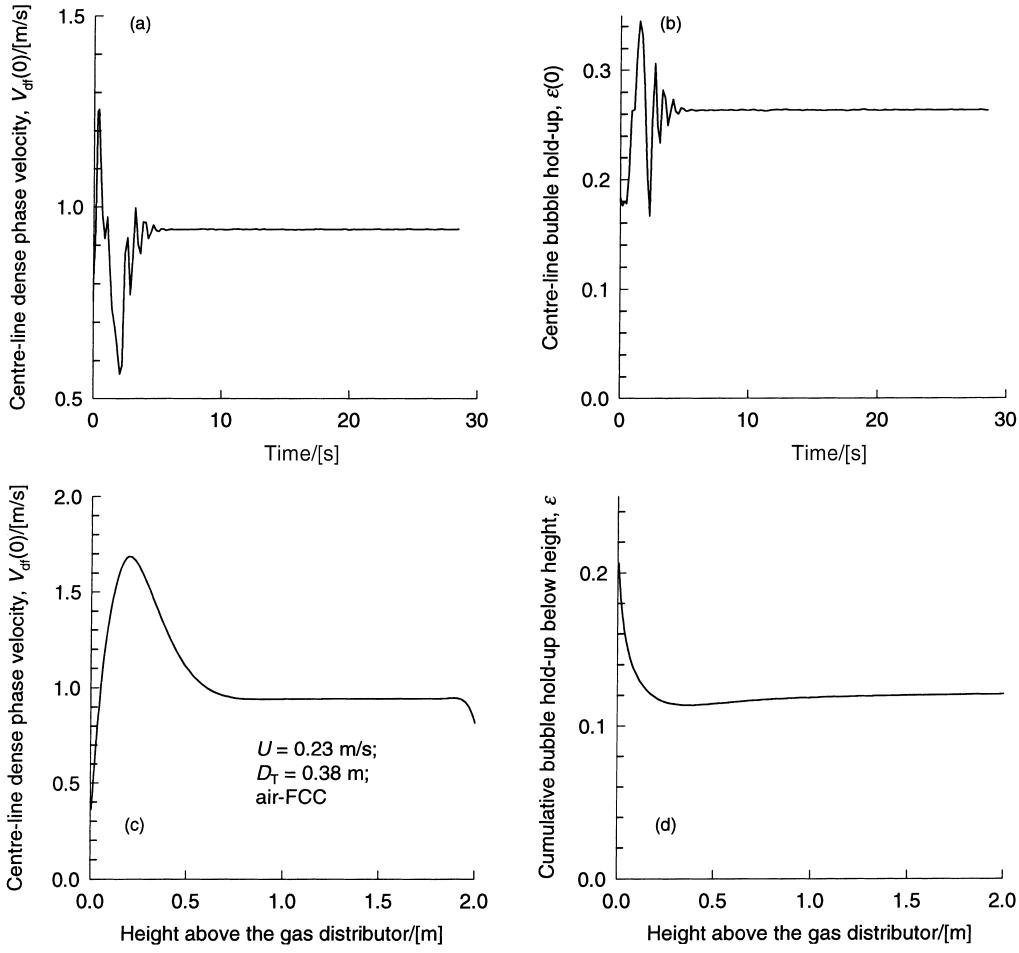

Fig. 7. Start up dynamics of 0.38 m diameter column. Also shown is the variation of properties along the dispersion height at steady-state.

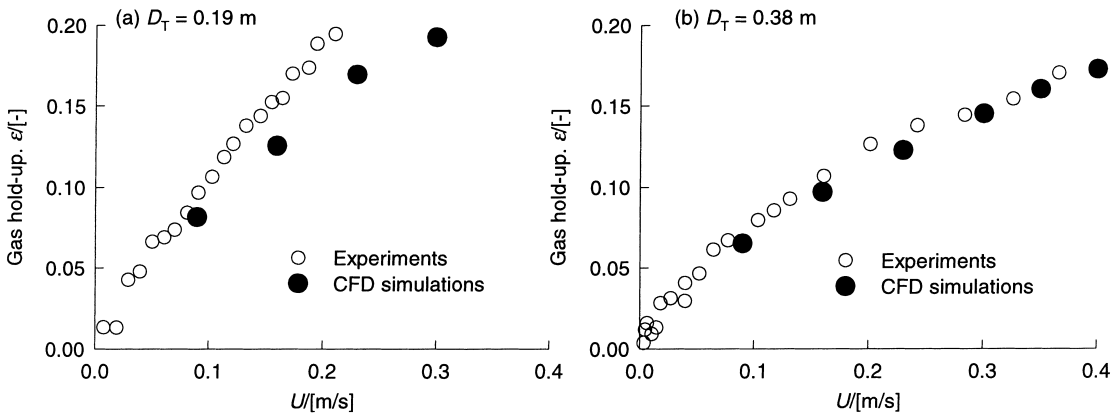

Fig. 8. Comparison of CFD simulations with experimental data on bubble hold-up.

hold-up distribution, the cumulative gas hold-up is virtually the same for the two types of simulations shown in Fig. 6 (0.119 for 2D versus 0.122 for 3D).

Having validated the accuracy of 2D axi-symmetric simulations we have used this strategy to simulate gas–solid fluid beds of various scales in order to study scale effects. The first issue concerns the choice of the computational grid. Anticipating steeper velocity gradients near the wall region and in the bottom portion of the column, a non-uniform grid was used. For the 0.19 and 0.38 m diameter columns, 30 grid cells in the radial direction were used; 10 grid cells in the central core and 20 grid cells towards the wall region. In the axial direction, the first 0.2 m bottom portion of the column consisted of 10 mm cells and the remainder 2.8 m height consisted of 20 mm cells. The total number of cells was 4800. The dilute phase gas was injected only at the inner 13 of the total number of 30 cells. For the larger columns the dilute phase gas was injected in the central 32 of the 75 cells in radial direction. This injection strategy was used because the dilute phase tends to concentrate in the centre of the column and the applied gas injection strategy helped achieve easier convergence. The computational grid for the 1.5, 2, 4 and 6 m columns are specified in Table 1. For the 6 m column, for example, the total number of grid cells used was $75 \times 710 = 53250$ cells. In the radial direction 75 cells were used and 710 in the axial direction. The time stepping strategy used in the transient simulations for attainment of steady state was: 20 iterations at 5×10^{-4} s, 20 iterations at 1×10^{-3} s, 460 iterations at 5×10^{-3} s, 2000 iterations at 1×10^{-2} s. The 0.19 and 0.38 m diameter column simulations were carried out on a Silicon Graphics Power Indigo workstation with an R8000 processor. Simulations of the 1.5, 2, 4 and 6 m diameter columns were carried out on a Power Challenge machine employing three R10000 processors in parallel. Each simulation was completed in about 36 h. In all the runs, steady state was reached within 15 s; this is illustrated in Fig. 7 which shows the centre-line velocity of the dense phase, $V_{df}(0)$, and the centre-line gas hold-up, at a height of 1.6 m above the distributor of the 0.38 m diameter fluid bed operating at $U - U_{df} = 0.23$ m/s. The sharp change in $V_{df}(0)$, after about 2 s is caused by the bubble "front" approaching the monitoring point. The centre-line liquid velocity $V_{df}(0)$, and cumulative gas hold-up vary along the column height in the region close to the distributor; see Fig. 7. However, for the large dispersion heights used the variations

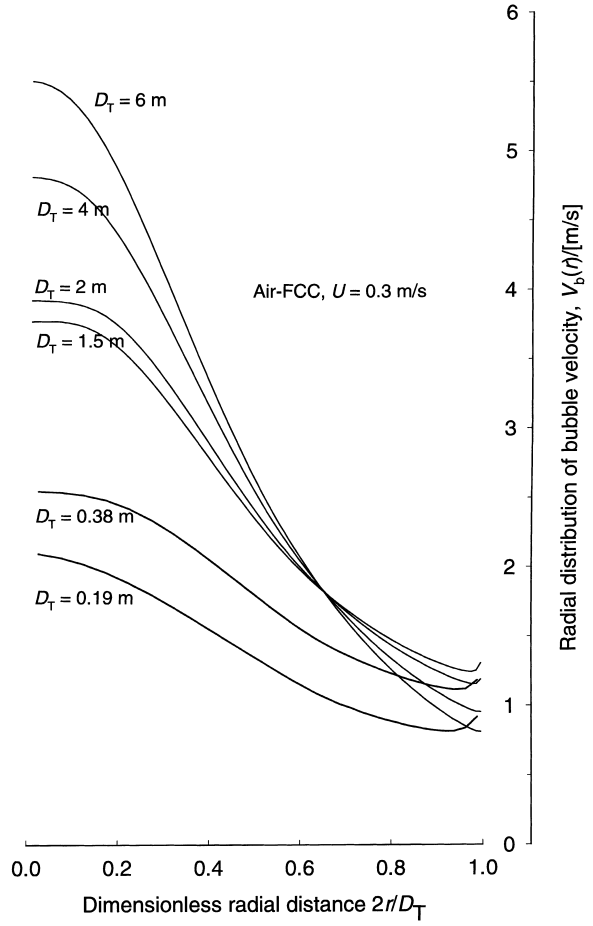

Fig. 9. Scale effect on the radial distribution of the bubble rise velocity.

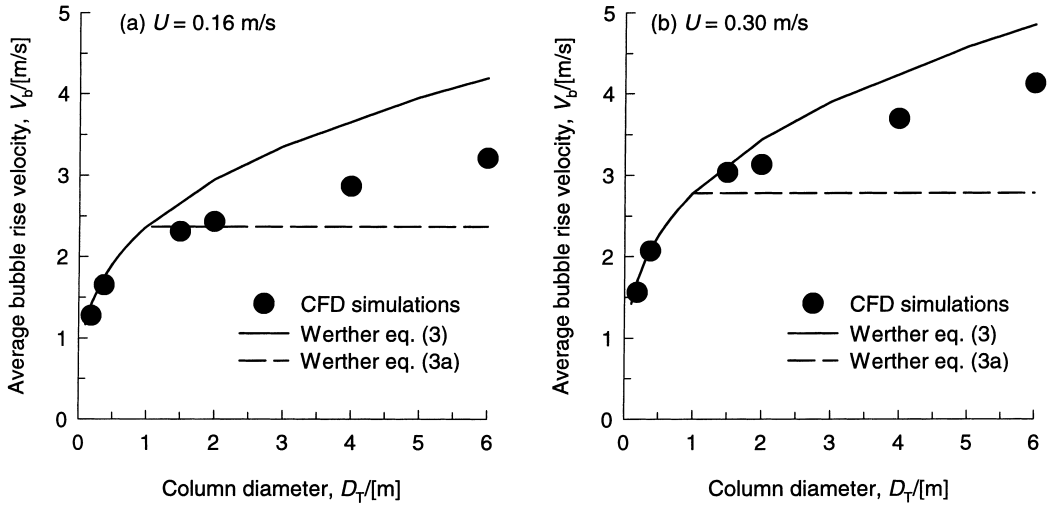

Fig. 10. Influence of column diameter on the average bubble rise velocity. Eulerian simulations compared with the Werther correlations (3) and (3a).

tend to even out. The reported $V_{df}(0)$, $V_{df}(r)$ and ε, are at the observation heights specified in Table 1.

The gas hold-up of the "dilute" phase determined from the CFD is compared with experimental data in Fig. 8. The agreement can be considered to be good. Having validated the Eulerian simulation model we may proceed to use CFD to study scale effects.

The most dramatic expression of the scale effect is noticed when we compare the bubble velocity distribution $V_b(r)$ as a function of the column diameter for a particular case, that of air–FCC operation at $U = 0.3$ m/s; see Fig. 9. The centre-line velocity $V_b(0)$ increases from about 2 m/s for a 0.19 m diameter column to 5.5 m/s for the 6 m diameter column.

The cross-sectional area average bubble velocity V_b, calculated from the $V_b(r)$ (and hold-up) profiles are shown in Fig. 10 as a function of column diameter for $U = 0.16$ and 0.3 m/s, respectively. The Eulerian simulations are compared with the Werther correlations, given by Eqs. (3) and (3a), with the bubble size calculated from Eq. (2) and taking $h_0 = 0.5$ m. The strong column diameter dependence of V_b on the column diameter anticipated by the Werther correlation is borne out by our Eulerian simulations. Our Eulerian simulation results for V_b, for $U = 0.16$ and 0.3 m/s, lie between the predictions of Eqs. (3) and (3a). The assertion of Werther (1992) that the value of ϑ remains constant beyond $D_T = 1$ m, is not supported by our simulations. On the other hand, the use of $\vartheta = 3.2 D_T^{0.33}$ for diameters larger than 1 m, predicts a higher value of V_b than obtained from Eulerian simulations. It appears that the scale dependence continually decreases with increasing column diameter; this result is also intuitively expected.

The average bubble hold-up, calculated from the Eulerian simulations is shown in Fig. 11 as a function of the column diameter. The strong decrease in bubble hold-up with increasing scale is evident.

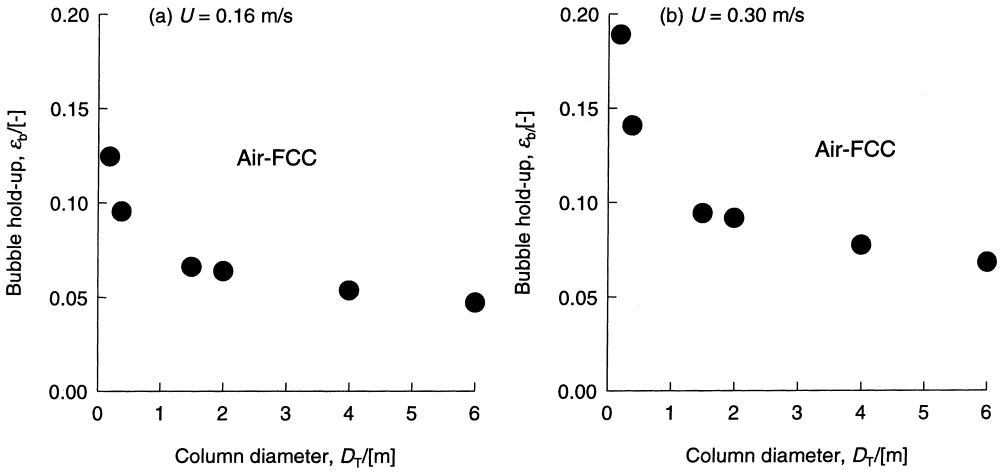

Fig. 11. Influence of column diameter on the average bubble hold-up obtained from Eulerian simulations.

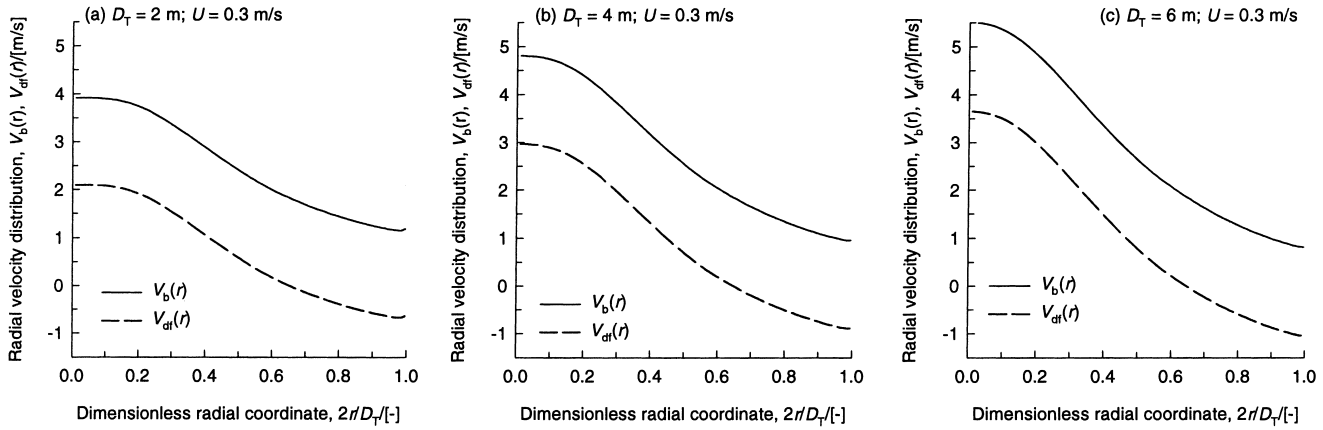

Fig. 12. Comparison of the radial distributions of dense phase velocity and bubble rise velocity for 2, 4 and 6 m diameter air–FCC columns operating at $U = 0.3$ m/s.

The fast-rising bubbles have the effect of carrying up the dense (emulsion) phase upwards in the central core of the column. When the bubbles disengage at the top, the dense phase is recirculated back to the bed. This recirculatory flow is predominantly in the wall region. The radial velocity distribution of the dense phase is shown in Fig. 12 for the 2, 4 and 6 m diameter columns, along with the bubble velocity distribution. The slip between the bubble and dense phases is the reason for the difference in the velocity of these phases at any radial position. A comparison of the $V_{df}(r)$ profiles for the three column diameter shows that the magnitude of the recirculatory flows increases with increasing column diameter. If the radial distribution of the dense phase velocity $V_{df}(r)$ is normalised with respect to the centre-line velocity $V_{df}(0)$ we see that the profiles coincide to a large extent; see Fig. 13. This suggests that the recirculatory flows can be characterised by a single parameter, the centre-line velocity $V_{df}(0)$. This centre-line velocity is a strong function of the column diameter and of the

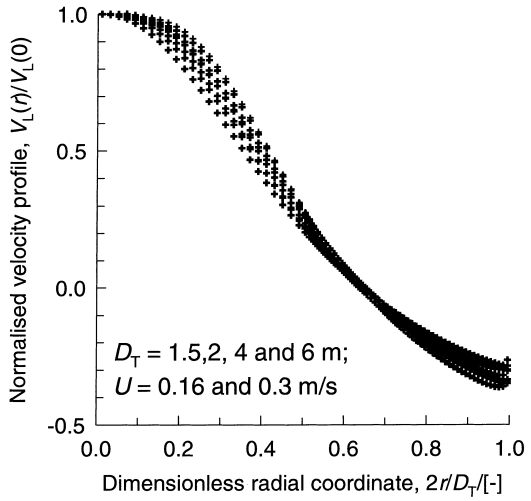

Fig. 13. Normalised dense phase velocity distribution for 1.5, 2, 4 and 6 m diameter air–FCC columns operating at $U = 0.16$ and 0.3 m/s.

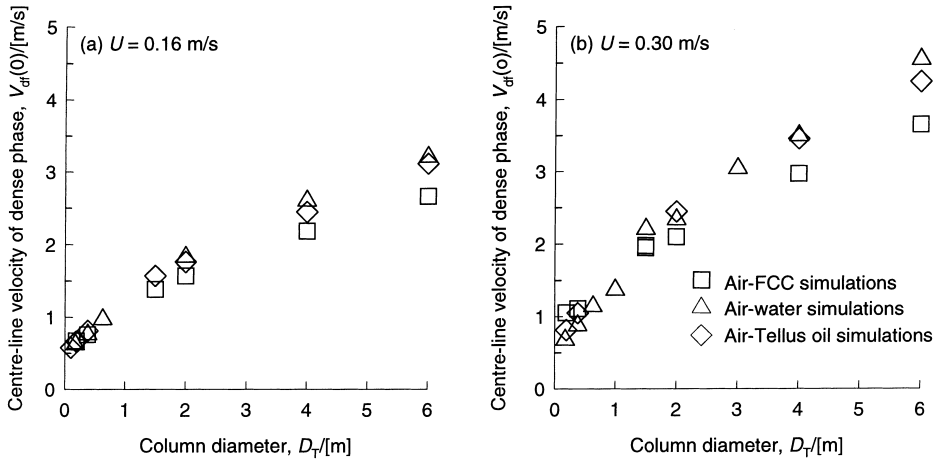

Fig. 14. Influence of column diameter on the centre-line dense phase velocity. Comparison of air–FCC with air–water and air–Tellus oil simulations published by Krishna et al. [38,39].

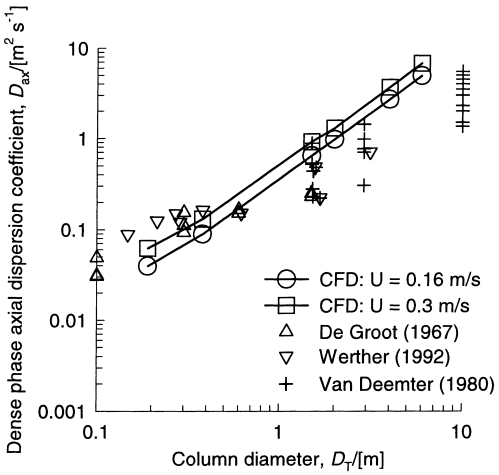

Fig. 15. Influence of column diameter on dense phase axial dispersion coefficient. Comparison of experimental data from literature [2,47,48] with D_{ax} predicted using Eq. (13), using the values of the centre-line velocity $V_{df}(0)$ from Eulerian simulations.

superficial gas velocity; see Fig. 14. In Fig. 14 we also compare the centre-line velocity $V_{df}(0)$ with the centre-line liquid velocity $V_L(0)$ obtained in gas–liquid bubble columns operating in the churn-turbulent regime with the air–water and air–Tellus oil systems; these bubble column simulations have been published earlier [38,39]. We note that the scale dependence of $V_{df}(0)$ for air–FCC is analogous to that of bubble columns.

In our previous work on Eulerian simulations of bubble columns with the air–water system [37,39] we had shown that the liquid phase backmixing coefficient D_{ax} can be calculated quite simply from a knowledge of the centre-line velocity using the formula

$$D_{ax} = 0.31 V_L(0) D_T \quad (13)$$

Asserting the analogy between gas–liquid bubble columns and gas–solid fluid beds, we can calculate the axial dispersion coefficient of the dense phase by using the Eulerian simulation results for $V_{df}(0)$. The calculations of D_{ax} using Eq. (13) are compared in Fig. 15 with the data culled from literature [2,47,48]. The agreement is good when we consider that the literature data has been obtained for a wide range of conditions with respect to superficial gas velocity, particle size and particle size distribution.

4. Conclusions

We have developed an Eulerian simulation model for gas–solid fluid beds with fine Geldart A powders assuming a constant bubble size. Using the two-fluid model with estimated pseudo "dense" phase properties, it is shown that CFD simulations of fluid beds can be carried out in manner analogous to that of gas–liquid bubble columns.

The agreement between experimental data in columns of 0.19 and 0.38 m diameter on bubble hold-up and CFD simulations gives us confidence in the use of CFD for scaling up purposes. Simulations of large diameter columns show the dramatic influence of column diameter on the bubble rise velocity; the predicted values are in broad agreement with the Werther correlation (3). A consequence of this is that the bubble hold-up is a significant decreasing function of the column diameter. The interfacial area for transfer from the bubble to emulsion phase will consequently decrease significantly with increasing column diameter; there is evidence in the published literature on a commercial scale fluid bed reactor in the Shell Chlorine Process tends to confirm this trend [3]. The simulation results also rationalise the published experimental data on backmixing of the dense phase. Further experimental verification of the predicted trends for gas hold-up by comparison with commercial scale data is required.

References

[1] D. Geldart (Ed.), Gas Fluidization Technology, Wiley, New York, 1986.
[2] J. Werther, Fluidized-bed reactors, in: B. Elvers, S. Hawkins, G. Schulz (Eds.), Ullmann's Encyclopedia of Industrial Chemistry, Vol. B4, Principles of Chemical Reaction Engineering and Plant Design, 5th Edition, VCH Verlagsgesellschaft mbH, Weinheim, 1992.
[3] R. Krishna, Analogies in multiphase reactor hydrodynamics, in: N.P. Cheremisinoff (Ed.), Encyclopedia of Fluid Mechanics, Suppl. 2, Advances in Multiphase Flow, Gulf Publishing, Houston, 1993, pp. 239–297 (Chapter 8).
[4] R. Krishna, J. Ellenberger, S.T. Sie, Reactor development for conversion of natural gas to liquid fuels: a scale up strategy relying on hydrodynamic analogies, Chem. Eng. Sci. 51 (1996) 2041–2050.
[5] R.M. Davies, G.I. Taylor, The mechanics of large bubbles rising through extended liquids and through liquids in tubes, Proc. Roy. Soc. London A200 (1950) 375–390.
[6] R. Clift, J.R. Grace, M.E. Weber, Bubbles, Drops And Particles, Academic Press, San Diego, 1978.
[7] J.F. Davidson, D. Harrison, R.C. Darton, R.D. LaNauze, The two-phase theory of fluidization and its application to chemical reactors, in: L. Lapidus, N.R. Amundson (Eds.), Chemical Reactor Theory, A Review, Prentice-Hall, Englewood Cliffs, NJ, 1977, pp. 583–685.
[8] L.S. Fan, K. Tsuchiya, Bubble Wake Dynamics in Liquids and Liquid–Solid Suspensions, Butterworth-Heinemann, Boston, 1990.
[9] G.B. Wallis, One-Dimensional Two-Phase Flow, McGraw-Hill, New York, 1969.
[10] L.S. Fan, C. Zhu, Principles of Gas–Solid Flows, Cambridge University Press, UK, 1998.
[11] R. Krishna, J.M. van Baten, M.I. Urseanu, J. Ellenberger, Rise velocity of single circular-cap bubbles in two-dimensional beds of powders and liquids, Chem. Eng. Process. 39 (2000) 433–440.
[12] R.C. Darton, R.D. LaNauze, J.F. Davidson, D. Harrison, Bubble growth due to coalescence in fluidized beds, Trans. Inst. Chem. Eng. 55 (1977) 274–280.
[13] J. Ellenberger, R. Krishna, A unified approach to the scaleup of gas–solid fluidized and gas–liquid bubble column reactors, Chem. Eng. Sci. 49 (1994) 5391–5411.
[14] R. Collins, The effect of a containing cylindrical boundary on the velocity of a large gas bubble in a liquid, J. Fluid Mech. 28 (1967) 97–112.

[15] D. Bhaga, M.E. Weber, In-line interaction of a pair of bubbles in a viscous liquid, Chem. Eng. Sci. 35 (1980) 2467–2474.
[16] I. Komasawa, T. Otake, M. Kamojima, Wake behaviour and its effect on interaction between spherical-cap bubbles, J. Chem. Eng. Jpn. 13 (1980) 103–109.
[17] R. Krishna, M.I. Urseanu, J.M. Van Baten, J. Ellenberger, Rise velocity of a swarm of large gas bubbles in liquids, Chem. Eng. Sci. 54 (1999) 171–183.
[18] R. Clift, J.R. Grace, Continuous bubbling and slugging, in: J.F. Davidson, R. Clift, D. Harrison (Eds.), Fluidization, 2nd Edition, Academic Press, London, 1985 (Chapter 3).
[19] M.N. Bogere, A rigorous description of gas–solid fluidized beds, Chem. Eng. Sci. 51 (1996) 603–622.
[20] A. Boemer, H. Qi, U. Renz, Eulerian simulation of bubble formation at a jet in a two-dimensional fluidized bed, Int. J. Multiphase Flow 23 (1997) 927–944.
[21] J. Ding, D. Gidaspow, A bubbling fluidization model using the kinetic theory of granular flow, AIChE J. 36 (1990) 523–538.
[22] G. Ferschneider, P. Mège, Eulerian simulation of dense phase fluidized beds, Revue de L'Institut Français du Pétrole 51 (1996) 301–307.
[23] D. Gidaspow, Multiphase Flow and Fluidization — Continuum and Kinetic Theory Descriptions, Academic Press, New York, 1994.
[24] J.T. Jenkins, S.B. Savage, A theory for the rapid flow identical, smooth, nearly elastic spherical particles, J. Fluid Mech. 130 (1983) 187–202.
[25] R. Krishna, J.M. Van Baten, J. Ellenberger, Scale effects in fluidized multiphase reactors, Powder Technol. 100 (1998) 137–146.
[26] J.A.M. Kuipers, K.J. van Duijn, F.P.H. van Beckum, W.P.M. van Swaaij, A numerical model of gas-fluidized beds, Chem. Eng. Sci. 47 (1992) 1913–1924.
[27] M. Syamlal, T.J. O'Brien, Computer simulation of bubbles in a fluidized bed, in: Proceedings of AIChE Symposium Series, No. 270, Vol. 85, 1989, pp. 22–31.
[28] B.G.M. Van Wachem, J.C. Schouten, R. Krishna, C.M. Van den Bleek, Eulerian simulations of bubbling behaviour in gas–solid fluidized beds, Comput. Chem. Eng. 22 (1998) S299–S306.
[29] B.G.M. Van Wachem, J.C. Schouten, R. Krishna, C.M. Van den Bleek, Validation of the Eulerian simulated dynamic behaviour of gas–solid fluidised beds, Chem. Eng. Sci. 54 (1999) 2141–2149.
[30] B.P.B. Hoomans, J.A.M. Kuipers, W.J. Briels, W.P.M. Van Swaaij, Discrete particle simulation of bubble and slug formation in a two-dimensional gas-fluidized bed: a hard sphere approach, Chem. Eng. Sci. 51 (1996) 99–118.
[31] M. Bauer, G. Eigenberger, A concept for multi-scale modeling of bubble columns and loop reactors, Chem. Eng. Sci. 54 (1999) 5109–5117.
[32] S. Grevskott, B.H. Sannæs, M.P. Dudukovic, K.W. Hjarbo, H.F. Svendsen, Liquid circulation, bubble size distributions, and solids movement in two- and three-phase bubble columns, Chem. Eng. Sci. 51 (1996) 1703–1713.
[33] H.A. Jakobsen, B.H. Sannæs, S. Grevskott, H.F. Svendsen, Modeling of bubble driven vertical flows, Ind. Eng. Chem. Res. 36 (1997) 4052–4074.
[34] R. Krishna, J.M. van Baten, Simulating the motion of gas bubbles in a liquid, Nature 398 (1999) 208–208.
[35] R. Krishna, M.I. Urseanu, J.M. Van Baten, J. Ellenberger, Wall effects on the rise of single gas bubbles in liquids, Int. Commn. Heat Mass Transfer 26 (1999) 781–790.
[36] R. Krishna, J.M. van Baten, Rise characteristics of gas bubbles in a 2D rectangular column: VOF simulations vs. experiments, Int. Commn. Heat Mass Transfer 26 (1999) 965–974.
[37] R. Krishna, M.I. Urseanu, J.M. Van Baten, J. Ellenberger, Influence of scale on the hydrodynamics of bubble columns operating in the churn-turbulent regime: experiments vs. Eulerian simulations, Chem. Eng. Sci. 54 (1999) 4903–4911.
[38] R. Krishna, J.M. Van Baten, M.I. Urseanu, Three-phase Eulerian simulations of bubble column reactors operating in the churn-turbulent flow regime: a scale up strategy, Chem. Eng. Sci. 55 (2000) 3275–3286.
[39] R. Krishna, M.I. Urseanu, J.M. van Baten, J. Ellenberger, Liquid phase dispersion in bubble columns operating in the churn-turbulent flow regime, Chem. Eng. J. 78 (2000) 43–51.
[40] A. Lapin, A. Lübbert, Numerical simulation of the dynamics of two-phase gas–liquid flows in bubble columns, Chem. Eng. Sci. 49 (1994) 3661–3674.
[41] Y. Pan, M.P. Dudukovic, M. Chang, Numerical investigation of gas-driven flow in 2-D bubble columns, AIChE J. 46 (2000) 434–449.
[42] J. Sanyal, S. Vasquez, S. Roy, M.P. Dudukovic, Numerical simulation of gas–liquid dynamics in cylindrical bubble column reactors, Chem. Eng. Sci. 54 (1999) 5071–5083.
[43] A. Sokolichin, G. Eigenberger, Applicability of the standard-turbulence model to the dynamic simulation of bubble columns. Part I. Detailed numerical simulations, Chem. Eng. Sci. 54 (1999) 2273–2284.
[44] J.G. Yates, Effect of temperature and pressure on gas–solid fluidization, Chem. Eng. Sci. 51 (1996) 167–205.
[45] C.M. Rhie, W.L. Chow, Numerical study of the turbulent flow past an airfoil with trailing edge separation, AIAA J. 21 (1983) 1525–1532.
[46] J. Van Doormal, G.D. Raithby, Enhancement of the SIMPLE method for predicting incompressible flows, Numer. Heat Transfer 7 (1984) 147–163.
[47] J.H. De Groot, Scaling-up gas-fluidized bed reactors, in: A.A.H. Drinkenburg (Ed.), Proceedings of the International Symposium on Fluidization, Netherlands University Press, Amstedam, 1967.
[48] J.J. Van Deemter, in: J.R. Grace, J.M. Matsen (Eds.), Proceedings of 5th International Conference on Fluidization, Henniker, New Hampshire, Plenum Press, New York, 1980.